Published online 27 May 2019

Nucleic Acids Research, 2019, Vol. 47, No. 13 ***6871–6884***
doi: 10.1093/nar/gkz458

Casein kinase 2 regulates telomere protein complex formation through Rap1 phosphorylation

Haruna Inoue, Mayuri Horiguchi, Kota Ono and Junko Kanoh*

Institute for Protein Research, Osaka University, Suita, Osaka 565-0871, Japan

Received September 08, 2018; Revised May 09, 2019; Editorial Decision May 11, 2019; Accepted May 14, 2019

ABSTRACT

Telomeres located at the ends of linear chromosomes play important roles in the maintenance of life. Rap1, a component of the shelterin telomere protein complex, interacts with multiple proteins to perform various functions; further, formation of shelterin requires Rap1 binding to other components such as Taz1 and Poz1, and telomere tethering to the nuclear envelope (NE) involves interactions between Rap1 and Bqt4, a nuclear membrane protein. Although Rap1 is a hub for telomere protein complexes, the regulatory mechanisms of its interactions with partner proteins are not fully understood. Here, we show that Rap1 is phosphorylated by casein kinase 2 (CK2) at multiple sites, which promotes interactions with Bqt4 and Poz1. Among the multiple CK2-mediated phosphorylation sites of Rap1, phosphorylation at Ser496 was found to be crucial for both Rap1–Bqt4 and Rap1–Poz1 interactions. These mechanisms mediate proper telomere tethering to the NE and the formation of the silenced chromatin structure at chromosome ends.

INTRODUCTION

Telomeres, the highly compacted chromatin structures at the ends of linear chromosomes, play crucial roles in genome stability. Telomere DNA contains species-specific repetitive sequences and commonly recruits shelterin, a protein complex that extends across double-strand (ds) telomere DNA and single-strand (ss) telomeric overhang DNA at chromosome ends (1). The major roles of shelterin are the protection of chromosome ends and the regulation of telomere DNA length. When formation of the shelterin complex is impaired, telomere DNA length becomes inappropriately short or long, and occasionally the chromosome ends fuse (2,3). Thus, this complex is crucial for telomere maintenance. However, the molecular mechanisms underlying the formation of the shelterin complex remain poorly understood.

In the fission yeast, *Schizosaccharomyces pombe*, telomeres are protected by the shelterin complex, which consists of six proteins, namely Taz1, Rap1, Poz1, Tpz1, Ccq1 and Pot1 (4). The association between shelterin and telomeres is mediated by the direct binding of Taz1 to telomeric dsDNA and Pot1 to ssDNA (5,6). Taz1 recruits Rap1 to telomeres, which in turn interacts with Poz1 to form the shelterin complex, which regulates telomere DNA length and protects chromosome ends (4,7,8). In addition, Rap1 directly binds to multiple proteins and is involved in various other telomere functions (9); for example, it associates with Bqt4, a nuclear membrane protein, to tether telomeres to the NE (10). During meiosis, Rap1 interacts with Bqt1 and Bqt2, which guide telomeres to the spindle pole body to form a meiosis-specific chromosome arrangement (11). Thus, Rap1 serves as a hub for various protein complexes at the telomeres in *S. pombe*.

Protein phosphorylation is a major regulatory mechanism *in vivo*. Casein kinase 2 (CK2), a highly conserved serine/threonine kinase that is constitutively active throughout the cell cycle, has many substrates and is involved in a variety of cellular processes such as DNA repair, cell-cycle control, cell survival, and transcriptional regulation (12–14). CK2-mediated phosphorylation affects protein–protein interactions. For example, the phosphorylation of Swi6, a homologue of heterochromatin protein 1 (HP1), by CK2 facilitates its interactions with other gene-silencing factors to mediate transcriptional repression at pericentromeric heterochromatin regions in *S. pombe* (15). Furthermore, it was reported that the CK2-mediated phosphorylation of human TRF1, a Taz1 homologue, is required for the efficient dimerization of TRF1, thereby promoting its association with telomeres (16).

Previously, we performed mass spectrometric analyses of *S. pombe* Rap1 and showed that it is highly phosphorylated *in vivo* and that a subset of these phosphorylation events is mediated by the Cdc2 kinase during M phase (17). Phosphorylation of Rap1 by Cdc2 was found to prevent its interaction with Bqt4, thereby facilitating the transient detachment of telomeres from the NE for precise chromosome segregation (17). We noted that some of the remaining phosphorylation sites in Rap1 matched the consensus sequences of CK2 phosphorylation (S/T-X-X-D/E) (18), al-

*To whom correspondence should be addressed. Tel: +81 6 6879 4328; Fax: +81 6 6879 4329; Email: jkanoh@protein.osaka-u.ac.jp

© The Author(s) 2019. Published by Oxford University Press on behalf of Nucleic Acids Research.
This is an Open Access article distributed under the terms of the Creative Commons Attribution Non-Commercial License (http://creativecommons.org/licenses/by-nc/4.0/), which permits non-commercial re-use, distribution, and reproduction in any medium, provided the original work is properly cited. For commercial re-use, please contact journals.permissions@oup.com

though any role for CK2 in telomere function had not previously been described in *S. pombe*. Here we report that CK2 directly phosphorylates Rap1 to facilitate the formation of shelterin and the tethering of telomeres to the NE by promoting Rap1 interactions with Bqt4 and Poz1.

MATERIALS AND METHODS

Strains, media and general techniques for *S. pombe*

The *S. pombe* strains used in this study are listed in Supplementary Table S1. Growth media and basic genetic and biochemical techniques were described previously (19–21).

In vitro kinase assay

A series of GST-Rap1 fusion proteins was purified from *Escherichia coli* using Glutathione Sepharose 4B (GE Healthcare Life Sciences). *Schizosaccharomyces pombe* Cka1-Flag was purified from *S. pombe* cell extracts in IP buffer (50 mM HEPES–KOH [pH 7.5]; 100 mM NaCl; 1 mM EDTA [pH 8.0]; 0.5% Triton X-100; 20 mM β-glycerophosphate; 0.1 mM Na_3VO_4; 50 mM NaF) using anti-Flag M2 affinity gel (Sigma, F2220). GST-Rap1 proteins were incubated with immunoprecipitated Cka1-Flag in kinase buffer (20 mM Tris–HCl [pH 7.5]; 10 mM $MgCl_2$; 1 mM EGTA; 2 mM DTT; 10 μM ATP, 10 μCi [γ-^{32}P] ATP) for 30 min at 30°C, and the proteins were analyzed by SDS-PAGE followed by autoradiography.

Mutagenesis

The phosphorylation sites of *rap1* were mutated to alanine- or glutamate-encoding codons using the QuickChange Lightning Site-Directed Mutagenesis Kit (Stratagene). To generate *rap1* mutant strains, *rap1*-null *S. pombe* cells (*rap1*::*ura4*$^+$) were transformed with DNA fragments containing a mutated allele of the *rap1*$^+$ open reading frame (ORF), and Ura- cells were selected on YES plates containing 5-fluoroorotic acid (5-FOA). The replacement of *ura4*$^+$ with the mutated *rap1*$^+$ was confirmed by PCR and genomic DNA sequencing.

Immunoprecipitation and phosphatase treatment

Logarithmically growing cells were collected by centrifugation and suspended in MASS buffer (25 mM HEPES–KOH [pH 7.5]; 200 mM NaCl; 10% glycerol; 0.1% NP-40). Zirconia beads were added, and the cells were broken by vortexing. Then, the insoluble debris was removed by centrifugation. Flag-tagged proteins were immunoprecipitated from the cell extracts using anti-Flag M2 affinity gel (Sigma, F2220). For phosphatase treatment, the Rap1–Flag-bound M2 affinity gel was washed twice with calf intestinal alkaline phosphatase (CIAP) buffer (50 mM Tris–HCl [pH 9.0]; 1 mM $MgCl_2$) and incubated in CIAP buffer with or without 60 U of CIAP (Takara) for 1 h at 30°C. The gels were then washed twice with MASS buffer and were subjected to western blot analysis.

Antibodies

Anti-Rap1-S496/S497-P antibodies were raised against SEK(pS)(pS)DDEEAFEKC peptides in rabbits. The antibodies were purified using a non-phosphorylated peptide column as a pre-absorption matrix followed by affinity purification using a phospho-peptide column (Sigma-Aldrich). Anti-Rap1 (17), anti-Flag (M2 F3165, Sigma), anti-HA (16B12, Covance or M180-3, Medical & Biological Laboratories) and anti-PSTAIR (P7962, Sigma) were used to detect Rap1, Flag-tagged and HA-tagged proteins, and Cdc2, respectively, by western blot analyses. Anti-Flag (M2 F3165, Sigma), anti-H3K9me2 (MABI 0307, MAB Institute) and anti-Swi6 (22) were used for ChIP analyses.

Yeast two-hybrid assay

The *rap1*$^+$ ORF was cloned into pACT2 (Clontech). The entire ORFs of *taz1*$^+$, *bqt4*$^+$ and *poz1*$^+$ were individually cloned into pGBKT7 (Clontech). To detect the interaction between Rap1 and Bqt1/Bqt2, pBridge-*bqt1*$^+$/*bqt2*$^+$ (11) was used. The *S. cerevisiae* strain Y190 (*MATa*, *ura3-52*, *his3-Δ200*, *lys2-801*, *ade2-101*, *trp1-901*, *leu2-3*, *112*, *gal4Δ*, *gal80Δ*, *LYS2*::*GAL1*$_{UAS}$-*HIS3*$_{TATA}$-*HIS3*, *URA3*::*GAL1*$_{UAS}$-*GAL1*$_{TATA}$-*lacZ*, *cyh*^{r}*2*) was used for β-galactosidase activity assays.

GST pull-down assay

A part of the *bqt4*$^+$ ORF corresponding to the amino acids 2–181 was amplified and cloned into pGEX-5X-2 (GE Healthcare). The *Escherichia coli* BL21-CodonPlus (Stratagene) was transformed with the plasmid, and the glutathione *S*-transferase (GST)-Bqt4 fusion protein was purified using Glutathione Sepharose 4B (GE Healthcare). GST or GST-Bqt4$_{2\text{-}181}$ proteins bound to glutathione beads were mixed with *S. pombe* cell extracts in TNE buffer (40 mM Tris–HCl [pH 7.5], 150 mM NaCl, 5 mM EDTA, 50 mM NaF, 20 mM β-glycerophosphate) at 4°C for 2 h and washed with TNE buffer. The protein complexes were boiled in SDS sample buffer and analyzed by SDS-PAGE, followed by immunoblotting and Coomassie Brilliant Blue (CBB) gel staining.

Measurement of the distance between the telomere and the NE

Telomeres, the NE, and microtubules were visualized with Taz1-mCherry, Ish1-GFP and GFP-Atb2, respectively. The distance between the telomeres and the NE was measured as previously described (10,17) (see Figure 4A). Cells in G_2 phase were subjected to the analyses of telomere-NE distances in interphase because *S. pombe* has a very short G_1 phase, and S phase occurs during cytokinesis.

Chromosome stability assay

Chromosome loss rate was measured using the Ch16 minichromosome as previously described (23). The loss rate per division was estimated using the following formula: loss rate $= 1-(F/I)^{1/N}$, where F and I are the final and initial percentages, respectively, of cells bearing Ch16 and N is the number of generations (24).

Chromatin immunoprecipitation (ChIP)

Exponentially growing cells were fixed at 32°C for 10 min in 1% formaldehyde and further fixed on ice for 50 min. Crude extracts were prepared by breaking the fixed cells in lysis buffer (50 mM HEPES–KOH [pH 7.5], 140 mM NaCl, 1 mM EDTA, 1% Triton X-100, 0.1% sodium deoxycholate, 1× cOmplete [Roche]) using a Multi-beads Shocker (Yasui Kikai), after which the chromatin was sheared by sonication using Bioruptor UCD-250 (BM Equipment) to an average genomic DNA length of <0.5 kb. The insoluble fraction of the crude extracts was removed by centrifugation, and the supernatant was immunoprecipitated using Dynabeads® M-280 anti-Mouse IgG (Thermo Fisher) as a carrier. The beads were washed twice with Buffer 1 (50 mM HEPES–KOH [pH 7.5], 140 mM NaCl, 1 mM EDTA, 1% Triton X-100, 0.1% sodium deoxycholate), twice with Buffer 1' (50 mM HEPES-KOH [pH 7.5], 500 mM NaCl, 1 mM EDTA, 1% Triton X-100, 0.1% sodium deoxycholate), twice with Buffer 2 (10 mM Tris–HCl [pH 8.0], 250 mM LiCl, 1 mM EDTA, 0.5% NP-40, 0.5% sodium deoxycholate), and twice with TE buffer (10 mM Tris–HCl [pH 8.0] and 1 mM EDTA). Immunoprecipitants and input extracts were treated with 10 μg/ml RNase A in TE buffer for 30 min at 37°C, then with 250 μg/ml proteinase K in 0.25% sodium lauryl sulfate (SDS) at 37°C overnight, followed by the reverse cross-linking reaction at 65°C for 6 h. Associated DNA fragments were purified by phenol chloroform extraction and ethanol precipitation, and then analyzed by quantitative PCR (q-PCR) using StepOne™ real-time PCR system (Thermo Fisher). Sequences of the primer sets for subsequent q-PCR are listed in Supplementary Table S2.

Southern blotting

To determine telomere lengths, genomic DNA (20 μg) was digested with ApaI, separated in 1% or 3% agarose gels, and analyzed on Hybond-N^+ nylon membranes (GE Healthcare Life Science). For the telomere and TAS1 probes, telomeric DNA and TAS1 fragments were excised from pAMP1 (25). To generate the rDNA probe for slot blot analyses, an rDNA fragment was amplified by PCR from *S. pombe* genomic DNA using the following primer set:

st144: 5′-CGCTAACCATTATTTACTGAGGAGAAC-3′

st150: 5′-ATCACCATATCCATATCCAATG-3′

The DNA fragments for probes were labelled with digoxigenin using the DIG High Prime DNA Labeling and Detection Starter Kit II (Roche).

Pulse-field gel electrophoresis (PFGE)

PFGE of NotI-digested chromosomal DNA was performed using a CHEF-DR III Pulsed Field Electrophoresis Systems (Bio-Rad) under the following conditions: 1% SeaKem Gold Agarose (Lonza) in 0.5× TBE; temperature, 10°C; initial switch time, 40 s; final switch time, 80 s; run time, 18 h; voltage gradient, 6.8 V/cm and angle, 120°.

RNA analyses

Total RNA was prepared from exponentially growing cells, followed by the treatment with recombinant DNase I (RNase-free) (TaKaRa Bio). For Reverse transcription (RT)-PCR, complementary DNA was synthesized using a High-Capacity cDNA Reverse Transcription Kit (Applied Biosystems) with random primers. RNA expression levels were analyzed by qPCR using the StepOne™ real-time PCR system (Thermo Fisher). Sequences of the primer sets used for q-PCR are listed in Supplementary Table S2.

RESULTS

Rap1 is phosphorylated by CK2 throughout the cell cycle

Previous mass spectrometric analyses of Rap1 immunoprecipitated from *S. pombe* cell extracts suggested the possibility that Rap1 is phosphorylated by CK2 in addition to Cdc2 (17). Therefore, we first examined whether CK2 can phosphorylate Rap1 *in vitro*. A series of Rap1 GST-fusion proteins was purified from *E. coli*, and *in vitro* kinase assays were performed with Flag-tagged Cka1 (a catalytic subunit of CK2), which was immunoprecipitaed from *S. pombe* cell lysates with (*ckb1*$^+$) or without Ckb1 (*ckb1*$^-$), a regulatory subunit of CK2. Fragments B, C and D, which cover amino acids 300–370, 360–520 and 510–580 of Rap1, respectively, were phosphorylated by CK2 in a Ckb1-dependent manner (Figure 1A). To determine the sites of Rap1 that were phosphorylated by CK2, serine or threonine residues (15 in total in fragments B–D) located in the consensus target sequence of CK2 (serine or threonine residues followed by acidic or phosphorylated amino acids at the +3 position) were substituted with alanine, a non-phosphorylatable amino acid. Combinational mutation analyses showed that fragment B, harboring mutations at Ser317 and Ser329, fragment C, with mutations at Ser484, Ser487, Ser496 and Ser497, and fragment D, with a mutation at Ser538, were not phosphorylated by CK2, whereas these fragments harboring other combinations of mutations were substrates of CK2 *in vitro* (Figure 1B–D). Thus, we identified Ser317, Ser329, Ser484, Ser487, Ser496, Ser497 and Ser538 of Rap1 as sites that are phosphorylated by CK2 *in vitro* (Figure 1E).

To determine whether Rap1 is phosphorylated by CK2 *in vivo*, the *rap1-7A* or *rap1-7E* mutants, in which the aforementioned seven potential phosphorylation sites were substituted with either non-phosphorylatable alanine or phospho-mimic glutamate, were generated. Then, Rap1 proteins were analyzed by western blotting wherein the phosphorylated form of Rap1 migrated slower than the unphosphorylated form (17). The Rap1-7A protein migrated faster than wild-type Rap1 or Rap1-7E proteins, suggesting that at least some of the seven serine residues are phosphorylated *in vivo* (Figure 2A). To more directly detect Rap1 phosphorylation, antibodies that recognize the phosphorylation of Ser496/Ser497 were produced (note that Ser496 is the most important amino acid residue that regulates the interaction between Rap1 and Bqt4 [see below]) (Figure 2A, Supplementary Figure S1A). The phospho-Ser496/Ser497-specific antibodies recognized the Rap1-Flag protein immunoprecipitated from *S. pombe* cell extracts; however, Rap1-Flag protein was barely detected after dephosphorylation by CIAP, demonstrating that Rap1 is indeed phosphorylated at Ser496/Ser497 *in vivo* (Figure 2B). Furthermore, Rap1 phosphorylation at Ser496/Ser497 was decreased by the inactivation of CK2 in the *orb5-19*

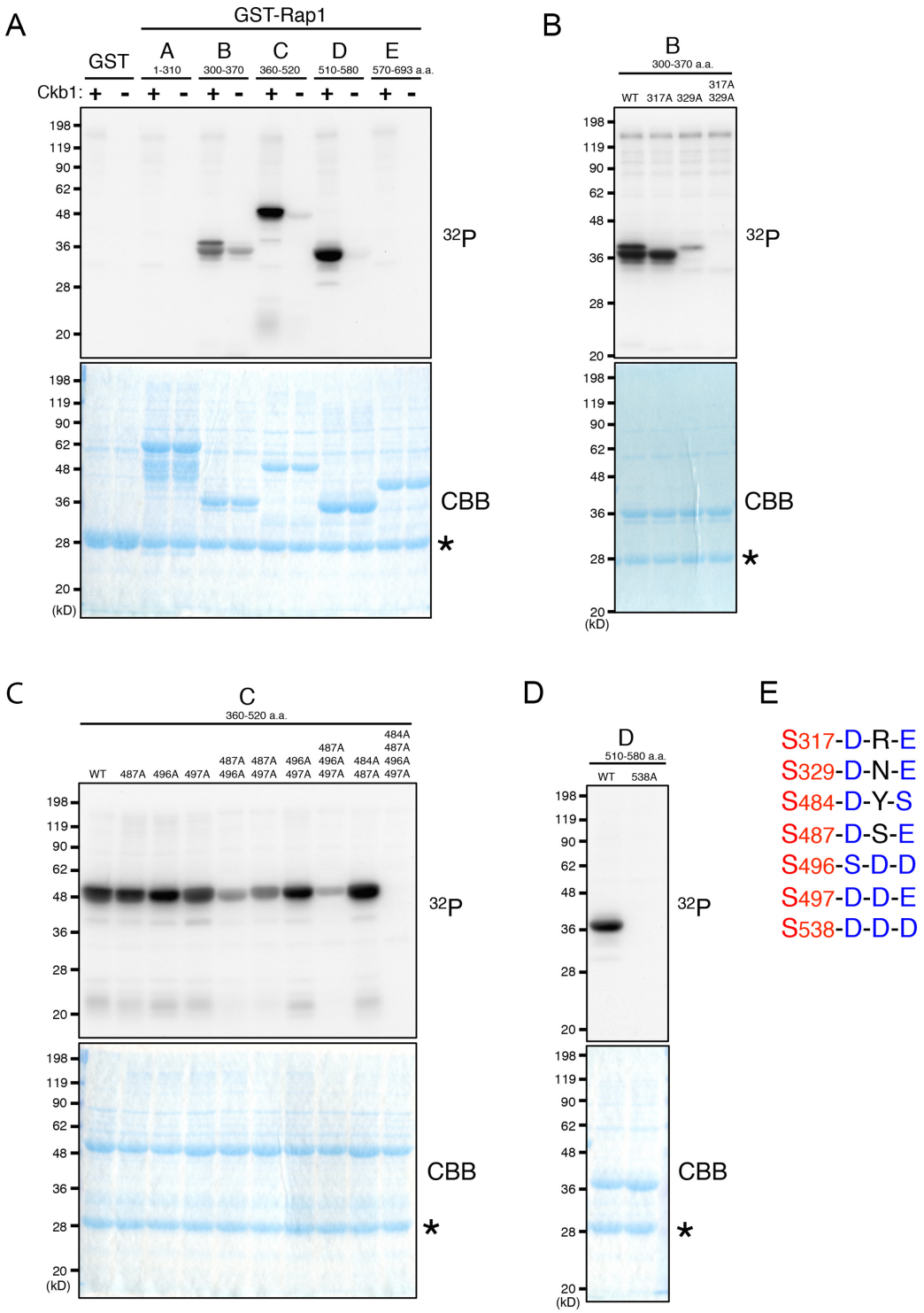

Figure 1. Rap1 is phosphorylated at seven serine residues by CK2 *in vitro*. (**A**) Rap1 phosphorylation by CK2 *in vitro*. *In vitro* kinase assays using GST-Rap1 proteins (fragments A–E) as substrates. A, 1–310 a.a.; B, 300–370 a.a.; C, 360–520 a.a.; D, 510–580 a.a.; E, 570–693 a.a. GST-Rap1 proteins were incubated with Cka1-Flag purified from *S. pombe* wild-type or *ckb1*$^{-}$ cells in the presence of γ-[^{32}P]ATP. Proteins were analyzed by SDS-PAGE. Autoradiography and Coomassie Brilliant Blue (CBB) staining of the gel are shown at the top (^{32}P) and the bottom (CBB). The asterisk indicates Cka1-Flag. (**B**) Mutation analyses of GST-Rap1-B. GST-Rap1-B proteins harbored single or double mutations at Ser317 and Ser329. An *in vitro* kinase assay was performed as in (A). Note that the upper and lower bands represent phosphorylation at Ser317 and Ser329, respectively. The double mutation at Ser317 and Ser329 completely abolished phosphorylation. (**C**) Mutation analyses of GST-Rap1-C. An *in vitro* kinase assay was performed as in (A). Note that the quadruple mutation at Ser484, Ser487, Ser496, and Ser497 completely abolished phosphorylation. (**D**) Mutation analysis of GST-Rap1-D. An *in vitro* kinase assay was performed as in (A). Note that the single mutation at Ser538 completely abolished phosphorylation. (**E**) Amino acid sequences of CK2 *in vitro* phosphorylation sites of Rap1. The phosphorylated serine residues are shown in red. Negatively charged amino acids (aspartate, glutamate, or phosphorylated serine) following the phosphorylated residues are shown in blue.

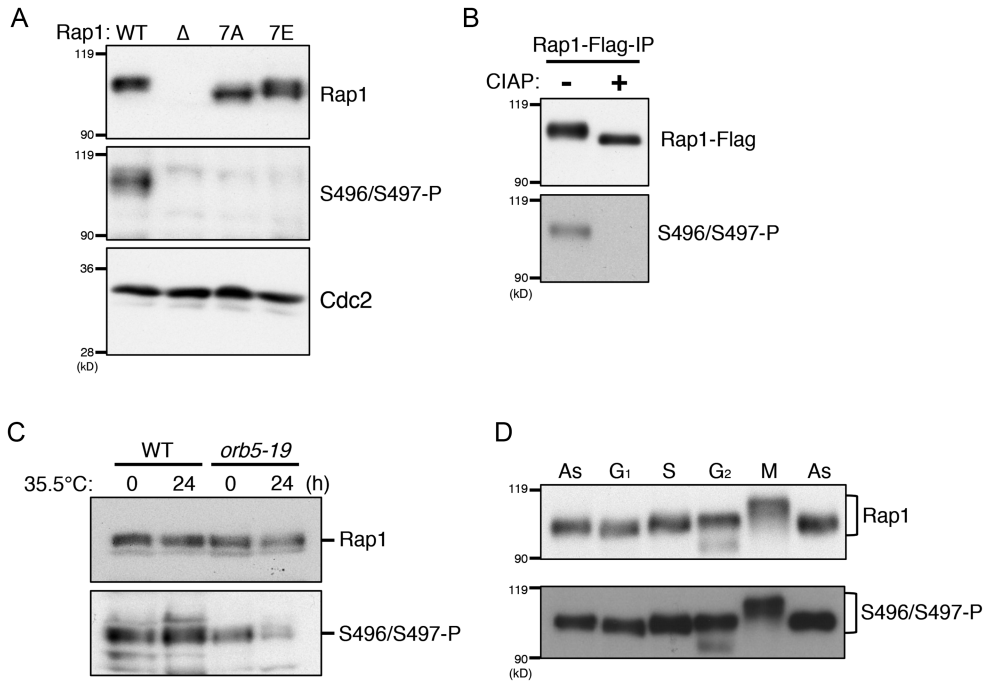

Figure 2. Rap1 is phosphorylated by CK2 throughout the cell cycle *in vivo*. (**A**) Band-shift analysis of Rap1-7A and Rap1-7E proteins. The whole cell extracts were prepared from wild-type (WT), *rap1*Δ, *rap1-7A*, and *rap1-7E* cells grown in YES at 32°C and were analyzed by western blotting using anti-Rap1, anti-phospho-Rap1, and anti-PSTAIR antibodies for Rap1 and Cdc2 (loading control), respectively. (**B**) Rap1 is phosphorylated at Ser496 and Ser497 *in vivo*. Immunoprecipitated Rap1-Flag proteins were incubated with or without CIAP for 1 h at 32°C and were analyzed by western blotting using anti-Flag and anti-phospho-Ser496/Ser497 antibodies. Note that the anti-phospho-Ser496/Ser497 antibody barely recognized the Rap1 protein that was dephosphorylated by CIAP. (**C**) Rap1 is phosphorylated at Ser496 and Ser497 in a CK2-dependent manner. Wild-type (WT) and *orb5-19* cells were grown at 25°C (the permissive temperature) until mid-log phase (0 h) and incubated at 35.5°C (the restrictive temperature) for 24 h. The whole cell extracts were analyzed by western blotting using anti-Rap1 and anti-phospho-Ser496/Ser497 antibodies. (**D**) Rap1 is constitutively phosphorylated at Ser496/Ser497 during the cell cycle. The wild-type strain was grown in YES at 32°C to mid-log phase (asynchronous, As). Strains *cdc10-129*, *cdc22-m45* and *cdc25-22* were grown in YES at 25°C to early log phase and then arrested in G_1, S or G_2 phase, respectively, by a temperature shift to 35.5°C for 4 h. Strain *nda3-KM311* was grown in YPD at 32°C and arrested in early M phase by a temperature shift to 20°C for 12 h. Rap1-2HA6His proteins were affinity purified and analyzed by immunoblotting using anti-Rap1 and anti- phospho-Ser496/Ser497 antibodies. Note that Rap1 is highly phosphorylated by Cdc2 in M phase, which appears as the shifted bands.

(cka1) mutant (26) (Figure 2C). These results indicate that Rap1 is phosphorylated by CK2 at multiple sites including Ser496/Ser497 *in vivo*. We also examined the timing of the phosphorylation at Ser497/Ser497 during the cell cycle using synchronized cells. Phosphorylation at Ser497/Ser497 was almost constant throughout the cell cycle (Figure 2D and Supplementary Figure S1A and B).

Rap1 phosphorylation by CK2 promotes Rap1–Bqt4 interactions

We next investigated the functions of Rap1 phosphorylation by CK2. Rap1 plays an important role as a hub for telomere protein complexes (9,17,27–29). The seven CK2 phosphorylation sites of Rap1 are located within or near the interaction domains of Rap1-partners (Figure 3A). We thus tested whether Rap1 phosphorylation affects the formation of telomere protein complexes using a yeast two-hybrid system. Strikingly, the *rap1-7A* mutation decreased the efficiency of Rap1 interactions with Bqt4, a nuclear membrane protein, whereas this mutation did not have a significant effect on interactions between Rap1 and the other Rap1-partners, including Taz1, Poz1, Bqt1 and Bqt2 (Figure 3B). Further, single point mutation analyses suggested that phosphorylation at Ser496 is critical for the Rap1–Bqt4 interaction (Figure 3C). It should be noted that Ser496 is located within the interface of the Bqt4-binding domain of Rap1 (490–513 a.a.) (29). Furthermore, Rap1-7A showed lower affinity for GST-Bqt4$_{2\text{-}181}$, compared to that of wild-type Rap1 or Rap1-7E, in *S. pombe* cell lysates (Figure 3D). These data indicate that Rap1 phosphorylation by CK2 promotes Rap1–Bqt4 interactions.

Rap1 phosphorylation at Ser496 facilitates telomere tethering to the NE

In *S. pombe*, telomeres are tethered to the NE during interphase, whereas they are transiently detached from the NE during mitosis for faithful chromosome segregation (17). Because the Rap1–Bqt4 interaction enables the tethering of telomeres to the NE, *bqt4*$^+$ or *rap1*$^+$ deletion results in substantial increases in telomere–NE distances during interphase (10,17). We thus examined whether Rap1 phosphorylation at Ser496 influences telomere tethering to the NE. To analyze the telomere position by microscopy, six telomeres of three chromosomes, along with the NE and microtubules were visualized with Taz1-mCherry, Ish1-GFP, and GFP-Atb2, respectively, and telomere–NE distances during

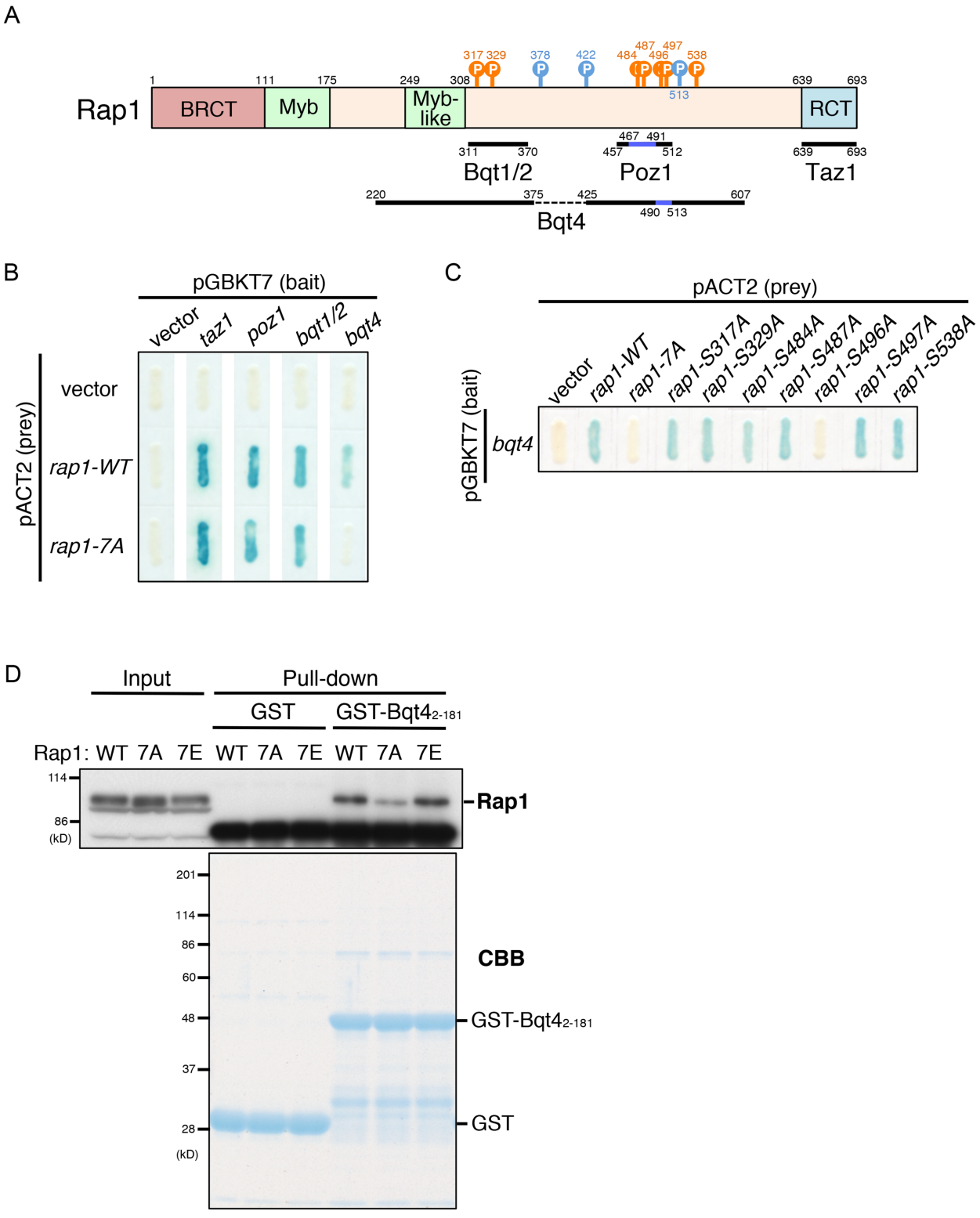

Figure 3. Rap1 phosphorylation by CK2 promotes the Rap1–Bqt4 interaction. (**A**) Schematic illustration of the Rap1 protein. Orange circles indicate seven CK2 phosphorylation sites, whereas blue circles indicate three Cdc2 phosphorylation sites (17). Black bars indicate binding domains to partner proteins revealed by yeast two-hybrid assays (9,17). Blue bars indicate the interaction surfaces with Poz1 and Bqt4 (27–29). Abbreviations for structural domains are as follows: BRCT, BRACA1 C terminus; Myb, Myb-related HLH (helix-loop-helix) motif; RCT, Rap1 C-terminal. (**B**) Rap1-7A is defective in its interactions with Bqt4. A budding yeast strain (Y190) was transformed with the plasmids indicated. β-galactosidase activity assays were performed using X-gal as substrates. (**C**) The S496A mutation has the strongest effect on Rap1–Bqt4 interaction. Yeast two-hybrid assays were performed as in (B) using the pACT2-*rap1*$^{+}$ plasmid containing a series of single mutations. (**D**) Rap1-7A, but not Rap1-7E, has a lower affinity for Bqt4 compared to wild-type Rap1. GST pull-down assays were performed using GST or GST-Bqt4 (2–181 a.a.) incubated with *S. pombe* cell extracts prepared from the wild-type, *rap1-7A*, or *rap1-7E* strains. The protein samples purified with glutathione beads were analyzed by western blotting using anti-Rap1 antibody (upper) and by CBB gel staining (lower).

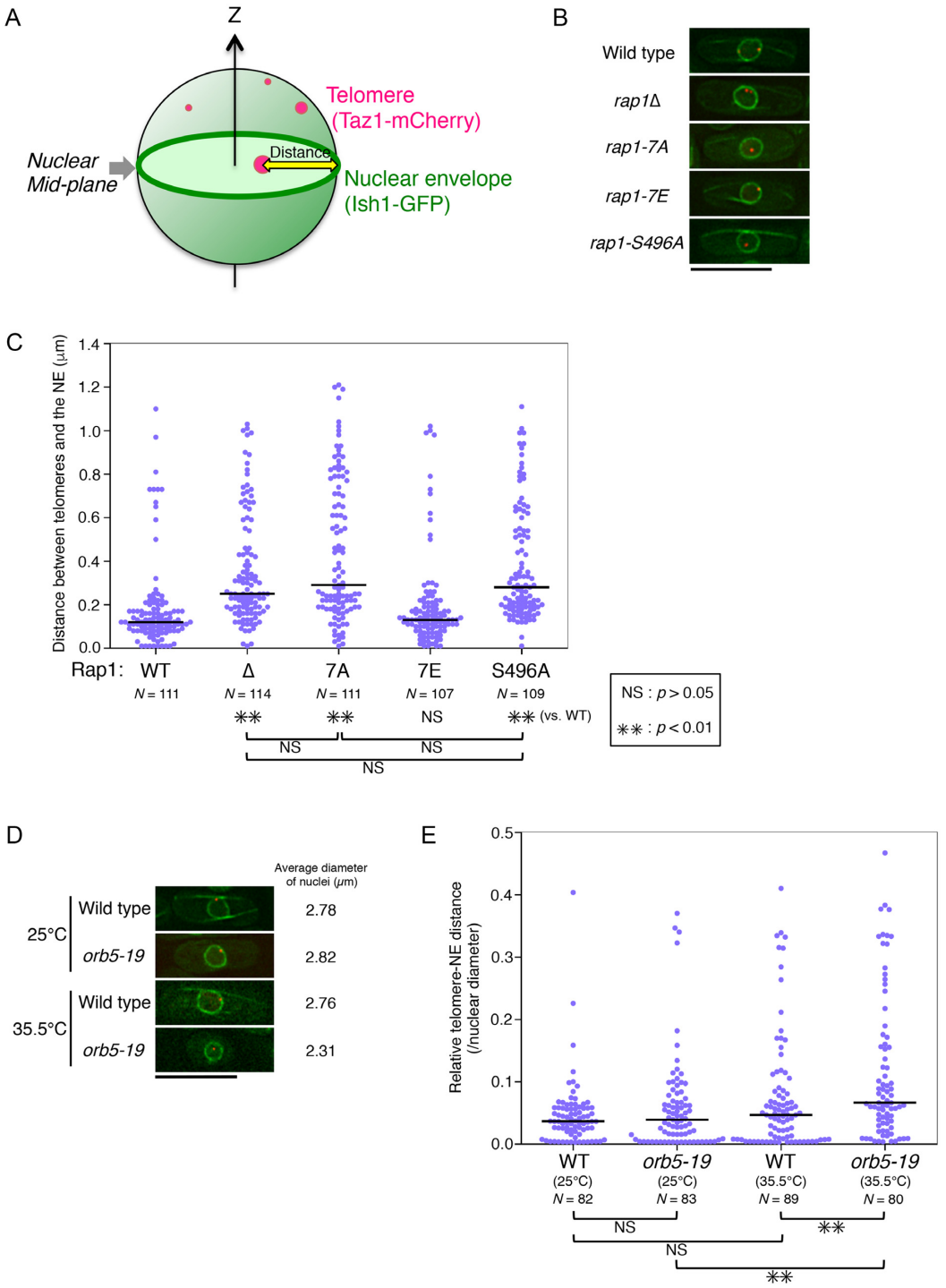

Figure 4. Rap1 phosphorylation by CK2 facilitates telomere tethering to the NE. (**A**) Schematic illustration of the method used to measure distances between telomeres and the NE. Telomeres, the NE, and microtubules were visualized with Taz1-mCherry, Ish1-GFP, and GFP-Atb2, respectively. Optical section data (13 focal planes with 0.3 μm spacing) were collected using a DeltaVision microscope system (Applied Precision) and were processed by a three-dimensional deconvolution method (37). Only the two-dimensional distance on a focal plane near the nuclear mid-plane was analyzed to ensure accurate measurements. Note that the telomeres of chromosome 3 (weak signals of Taz1-mCherry) are located in the nucleolus, and thus only the telomeres of chromosomes 1 and 2 (bright signals of Taz1-mCherry due to the clustering of telomeres) were analyzed. (**B**) Examples of images of wild-type, *rap1*Δ, *rap1-7A*, *rap1-7E* and *rap1-S496A* cells in G_2 phase. Shown are deconvolved images of the nuclear mid-plane. Bar, 10 μm. (**C**) Scatterplots of the distances between telomeres and the NE during G_2 phase. Cells were grown in EMM medium at 26°C. Bars in the graph indicate the median distances. *p*, Mann–Whitney U test. NS (not significant), $p > 0.05$; $^{**}p < 0.01$. (**D**) Examples of images of wild-type and *orb5-19* cells in G_2 phase. Shown are deconvolved images of the mid-plane of the nucleus. Bar, 10 μm. (**E**) Scatterplots of the relative distances between telomeres and the NE during G_2 phase normalized with each nuclear diameter. Cells were grown in YES medium at 25°C (the permissive temperature) or 35.5°C (the restrictive temperature) for 8 h. Bars in the graph indicate the median distances (0.037 [WT 25°C], 0.039 [*orb5-19* 25°C], 0.047 [WT 35.5°C] and 0.066 [*orb5-19* 35.5°C]. *p*, Mann–Whitney U test. NS, $p > 0.05$; $^{**}p < 0.01$.

interphase (G_2 phase) were measured as previously reported (17) (Figure 4A). In the wild-type strain (WT), the telomeres remained in the vicinity of the NE during interphase, and most telomeres were <0.2 μm from the NE (median, 0.12 μm), whereas the deletion of *rap1*$^+$ (*rap1*Δ) resulted in substantial increases in these distances (median, 0.25 μm). Intriguingly, the distances were also markedly larger in the *rap1-7A* mutant strain than in the wild type (median, 0.29 μm). In contrast, the distances in the *rap1-7E* mutant strain were comparable to those in the wild type (median, 0.13 μm). Furthermore, the distances in the *rap1-S496A* mutant in which Ser496 was substituted with alanine were larger than those in the wild type and comparable to those in the *rap1*Δ and *rap1-7A* strains (median, 0.28 μm; Figure 4B and C). Moreover, the *orb5-19* mutant, when measurements were normalized for decreased nuclear size (Figure 4D), exhibited relative distances larger than those in the wild-type strain at the restrictive temperature (median, 0.066 [relative to the nuclear diameter] and 0.16 μm [actual distance] versus 0.047 and 0.13 μm in the wild type) (Figure 4E). These data indicate that the phosphorylation of Rap1 by CK2 is important for telomere tethering to the NE, with Ser496 being a critical site, which increases the interaction with Bqt4.

In *S. pombe*, detachment of telomeres from the NE in M phase is important for normal movements and faithful segregation of chromosomes (17). To examine if the *rap1-7E* mutation causes constitutive attachment of telomeres to the NE and thereby interferes with normal chromosome segregation, cell growth and chromosome stability were analyzed. On rich medium, *rap1-7E* cells showed similar growth to wild-type and *rap1-7A* cells. Moreover, minichromosome (Ch16) stability was almost the same in *rap1-7E* and wild-type cells (Supplementary Figure S2). These data suggest that mechanisms, other than Rap1 phosphorylation by CK2, play dominant roles in regulating telomere localization in M phase.

Rap1 phosphorylation promotes Rap1–Poz1 interactions

Some of the CK2 phosphorylation sites in Rap1 are located within or near the Poz1-binding region of Rap1 (9,27,28) (Figure 3A). We thus examined whether Rap1 phosphorylation affects Rap1–Poz1 interactions *in vivo*. In the yeast two-hybrid assay, the *rap1-7A* mutation did not cause any obvious changes in Rap1–Poz1 interactions (Figure 3B). However, in *S. pombe* cell extracts, Rap1-7A barely associated with Poz1-Flag, whereas wild-type Rap1 and Rap1-7E were efficiently co-immunoprecipitated (Figure 5A). In contrast, Rap1-7A showed only slightly decreased association with Taz1 compared with the wild-type Rap1 or Rap1-7E (Figure 5B). These data indicate that the Rap1 phosphorylation by CK2 specifically promotes Rap1–Poz1 interactions *in vivo*.

We next examined whether the localization of Poz1 at telomeres is influenced by Rap1 phosphorylation. Chromatin immunoprecipitation (ChIP) assays revealed that Poz1 localization to telomeres was markedly decreased in the *rap1-7A* mutant, but not in the *rap1-7E* mutant, compared to that in the wild type (Figure 5C). These data suggest that the Rap1 phosphorylation by CK2 is important for the Rap1–Poz1 interaction and consequently for the normal localization of Poz1 to telomeres. Further analyses of single alanine mutants showed that the *rap1-S496A* mutation, which is located near the Poz1-binding interface of Rap1 (Figure 3A), caused the largest decrease in Poz1 localization, whereas all other single mutations caused a subtle decrease in Poz1 localization to the telomeres, as compared to that in the wild-type strain (Figure 5C). These data suggest that Rap1-Ser496 is the most important phosphorylation site for Poz1 localization to the telomeres.

Rap1 phosphorylation promotes the stable localization of shelterin components at telomeres and subtelomeres

Shelterin is a protein complex that consists of at least six subunits (4) (Figure 6A). A number of direct interactions among these six subunits have been reported (4,9,27,28,30–32), and the Rap1–Poz1 interaction is critical for the shelterin formation (27,28). We thus examined whether the *rap1-7A* mutation also influences the telomeric localization of shelterin components other than Poz1. ChIP analyses showed that the localization of all shelterin components was decreased by the *rap1-7A* mutation (Figure 6B and Supplementary Figure S3A and B). These data suggest that Rap1 phosphorylation by CK2 plays an important role in the recruitment of shelterin subunits and complex formation at the telomeres. It should be noted that the localization of Taz1 and Pot1, which directly bind to ds- and ss-telomere DNA, respectively, was also reduced by the *rap1-7A* mutation (Figure 6B). This suggests that the binding of Taz1 and Pot1 to dsDNA and ssDNA alone is insufficient to retain these proteins at telomeres, and that interactions with other shelterin components contribute to their stable localization.

It was reported that Taz1 is localized at the telomere-proximal regions of subtelomeres for approximately 10 kb (22); however, the subtelomeric localization of the other shelterin components is unknown. Intriguingly, ChIP analyses revealed that all of the shelterin components were localized at the telomere-proximal regions of subtelomeres for >10 kb in wild-type cells (Figure 6C). In the *rap1-7A* mutant, the subtelomeric localization of shelterin components was considerably decreased (Figure 6C). These results indicate that the Rap1 phosphorylation by CK2 plays an important role in the stable localization of shelterin components to both telomeres and subtelomeres.

Rap1 phosphorylation contributes to the maintenance of telomere DNA length

We next examined whether the considerable decrease in shelterin components at telomeres and subtelomeres in the *rap1-7A* mutant affects biological activities. Surprisingly, the *rap1-7A* mutant did not show obvious defects in the protection of chromosome ends (Supplementary Figure S4A), indicating that minimal shelterin localization to telomeres is sufficient for the protection of chromosome ends. In contrast, the *rap1-7A* mutant exhibited longer telomere DNA (∼310 bp) compared with the wild-type and *rap1-7E* strains (∼250 and 280 bp, respectively), indicating that the stability of shelterin localization affects the telomere length regulation (Figure 7A and B). The *orb5-19* mutant showed further longer telomere DNA (∼370 and 360 bp at permissive and

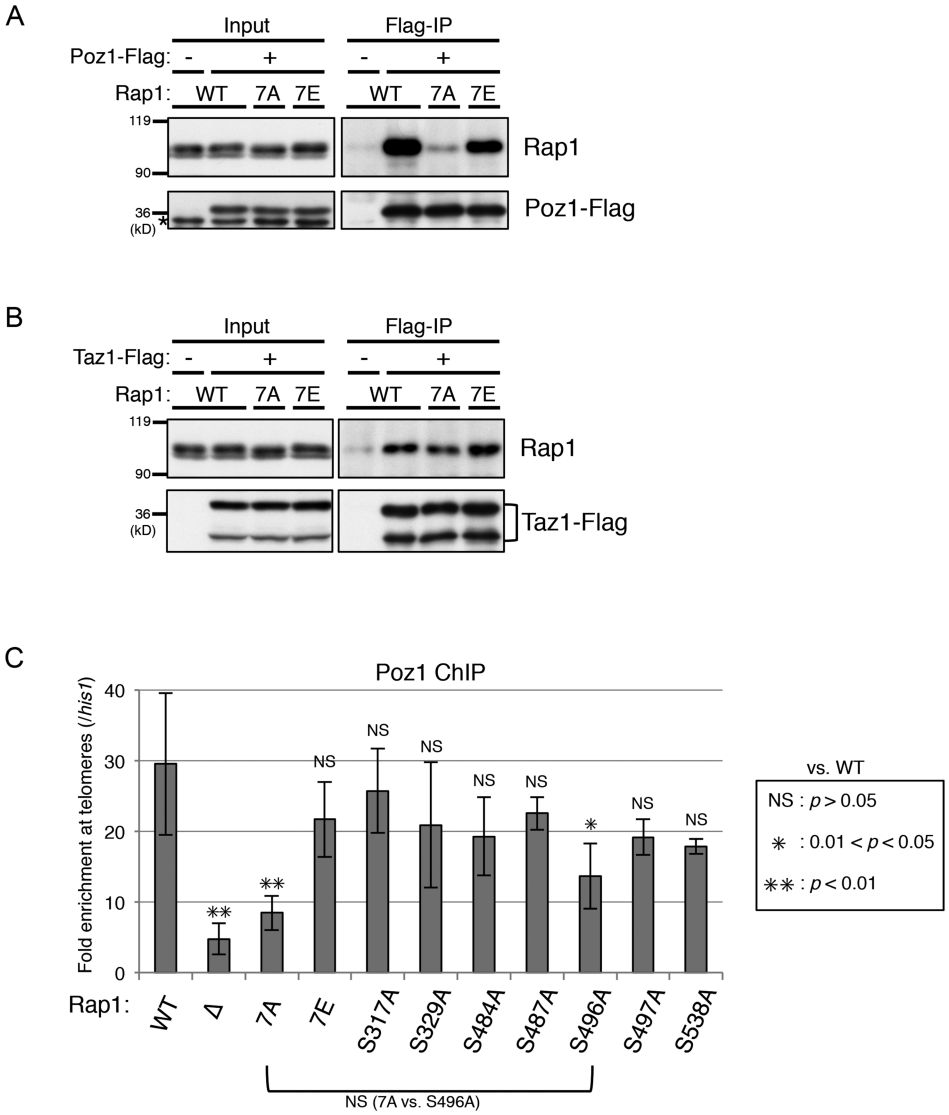

Figure 5. Rap1 phosphorylation by CK2 promotes the Rap1-Poz1 interaction at telomeres. (**A**) Rap1 phosphorylation by CK2 promotes the Rap1–Poz1 interaction *in vivo*. Poz1-Flag was immunoprecipitated from cell extracts of the wild-type or *poz1-flag* strains harbouring *rap1*$^{+}$, *rap1-7A* and *rap1-7E*. Immunoprecipitated samples were analyzed by immunoblotting using anti-Rap1 and anti-Flag antibodies. An asterisk indicates the position of non-specific bands. (**B**) Substantial Rap1-Taz1 interaction is maintained in *rap1-7A*. Taz1-Flag was immunoprecipitated from cell extracts of the wild-type or *taz1-flag* strains harbouring *rap1*$^{+}$, *rap1-7A*, and *rap1-7E*. Immunoprecipitated samples were analyzed by immunoblotting using anti-Rap1 and anti-Flag antibodies. (**C**) Rap1 phosphorylation promotes the localization of Poz1 at telomeres. Poz1-Flag localization at telomeres was determined by ChIP analyses followed by q-PCR. Fold enrichment at telomeres (detected by the primer set: jk1333 and jk1334) relative to the *his1* locus is shown. Error bars indicate the s.d. $N > 3$. *p*, Student's *t*-test (versus wild type or between *7A* and *S496A*). NS, $p > 0.05$; $0.01 < {*}p < 0.05$; ${**}p < 0.01$.

restrictive temperatures, respectively), suggesting the possibility that CK2 targets multiple telomere proteins including Rap1 (Figure 7C).

We next examined whether the telomeres in *rap1-7A* are maintained by telomerase via residual shelterin or by recombination. We found that telomere DNA length in *rap1-7A* was not affected by deletion of Rad22 (a Rad52 homolog) and that the frequency of formation of Rad22 foci was only slightly increased in *rap1-7A* compared with the wild type (Supplementary Figure S4B and C). Moreover, a telomere-proximal subtelomeric region, TAS1, was not amplified in *rap1-7A* (Supplementary Figure S4D), indicating that the telomere DNA in *rap1-7A* is not maintained by recombination. These data indicated that the Rap1 phosphorylation by CK2, although not essential, does contribute to the maintenance of telomere DNA length by telomerase.

Rap1 phosphorylation promotes formation of the silenced chromatin structure of chromosome ends

Telomeres form compact structures (33,34). In *S. pombe*, formation of the condensed chromatin at chromosome ends can be monitored by transcriptional gene silencing at the telomere-proximal subtelomeric region. Deletion of *rap1*$^{+}$ or *poz1*$^{+}$ resulted in the striking de-repression of the subtelomeric genes, *tlh1*$^{+}$ and *tlh2*$^{+}$ (*tlh1/2*$^{+}$), which are located approximately 10 kb from the telomeres of chromosomes 1

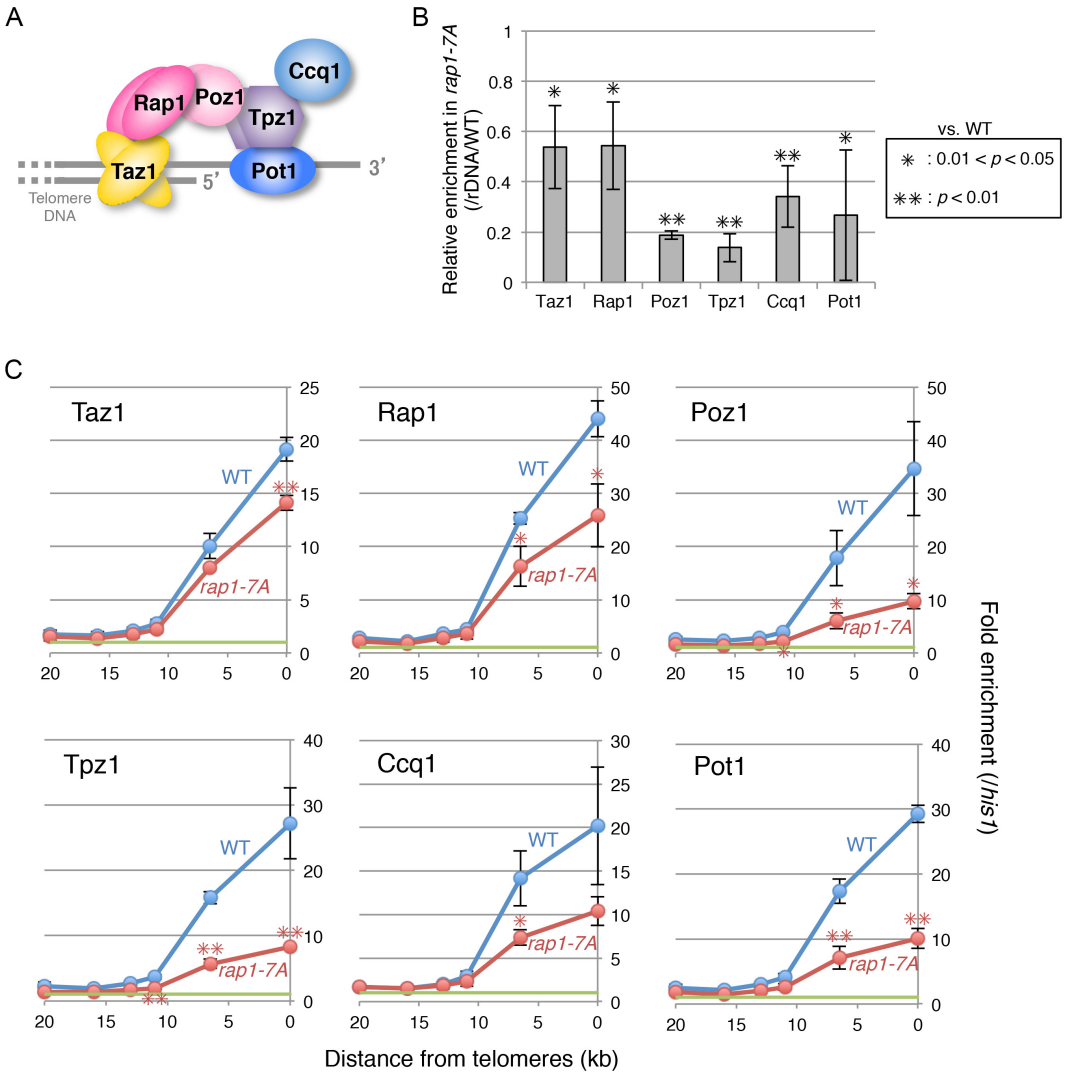

Figure 6. Rap1 phosphorylation by CK2 promotes the localization of shelterin components at telomeres and subtelomeres. (**A**) Schematic illustration of the *S. pombe* shelterin complex. (**B**) The association of shelterin components with telomeres is decreased in the *rap1-7A* mutant. ChIP analyses of Flag-tagged shelterin proteins. Telomere DNA and rDNA were detected by the Southern analyses. Representative data of slot Southern blots are shown in Supplementary S3B. Fold enrichment at telomeres relative to the rDNA loci in *rap1-7A* compared with that in wild type is shown. Error bars indicate the s.d. $N = 3$. p, Student's t-test (versus wild type). $0.01 < *p < 0.05$; $**p < 0.01$. (**C**) The association of shelterin components with subtelomeres is decreased in the *rap1-7A* mutant. ChIP analyses of Flag-tagged shelterin proteins followed by q-PCR. Blue dots indicate the values of wild type, whereas red dots are *rap1-7A*. Fold enrichment at subtelomeres relative to the *his1* locus is shown. Error bars indicate the s.d. $N = 3$. Green bars indicate 1 on the Y axis, which indicates no enrichment. p, Student's t-test (versus wild type) for the data at 0.2, 6.5 and 11 kb from telomeres. No mark, $p > 0.05$; $0.01 < *p < 0.05$; $**p < 0.01$.

and 2, respectively, indicating that the formation of shelterin is important for subtelomeric gene silencing as previously suggested (9,22) (Figure 8A). We then examined whether the introduction of the *rap1-7A* mutation causes defects in gene silencing at subtelomeric regions. A >10-fold increase in *tlh1/2*$^+$ RNA expression was observed in the *rap1-7A* mutant compared to that in the wild type, whereas a relatively small increase was noted in the *rap1-7E* mutant (Figure 8B). The *orb5-19* mutant also showed a striking increase of *tlh1/2*$^+$ RNA expression especially at the restrictive temperature (Figure 8C). Analyses of *rap1* single alanine mutations showed that mutations located near the Poz1-binding interface of Rap1 (Figure 3A), specifically *rap1-S496A* and *S497A*, caused a relatively high increase in *tlh1/2*$^+$ expression, as compared to those in the other single mutations (Figure 8B). Furthermore, deletion of *bqt4*$^+$, which causes telomere detachment from the NE, did not result in derepression of the *tlh1/2*$^+$ genes (Figure 8D). Moreover, the subtelomeric localization of methylated H3K9 and Swi6, an HP1 homologue, was not changed in the *rap1-7A* mutant, although the localization of Ccq1, which is one of the factors that establish heterochromatin at subtelomeres (35), was moderately reduced (Figures 6C and 8E). One possibility is that the RNAi machinery can utilize a part (the *dh* sequence) of RNA transcribed from the *tlh1/2*$^+$ loci and efficiently establishes heterochromatin in the Ccq1-depleted condition (22). These data indicate that the alleviation of subtelomeric gene silencing in *rap1-7A* is not due to the de-

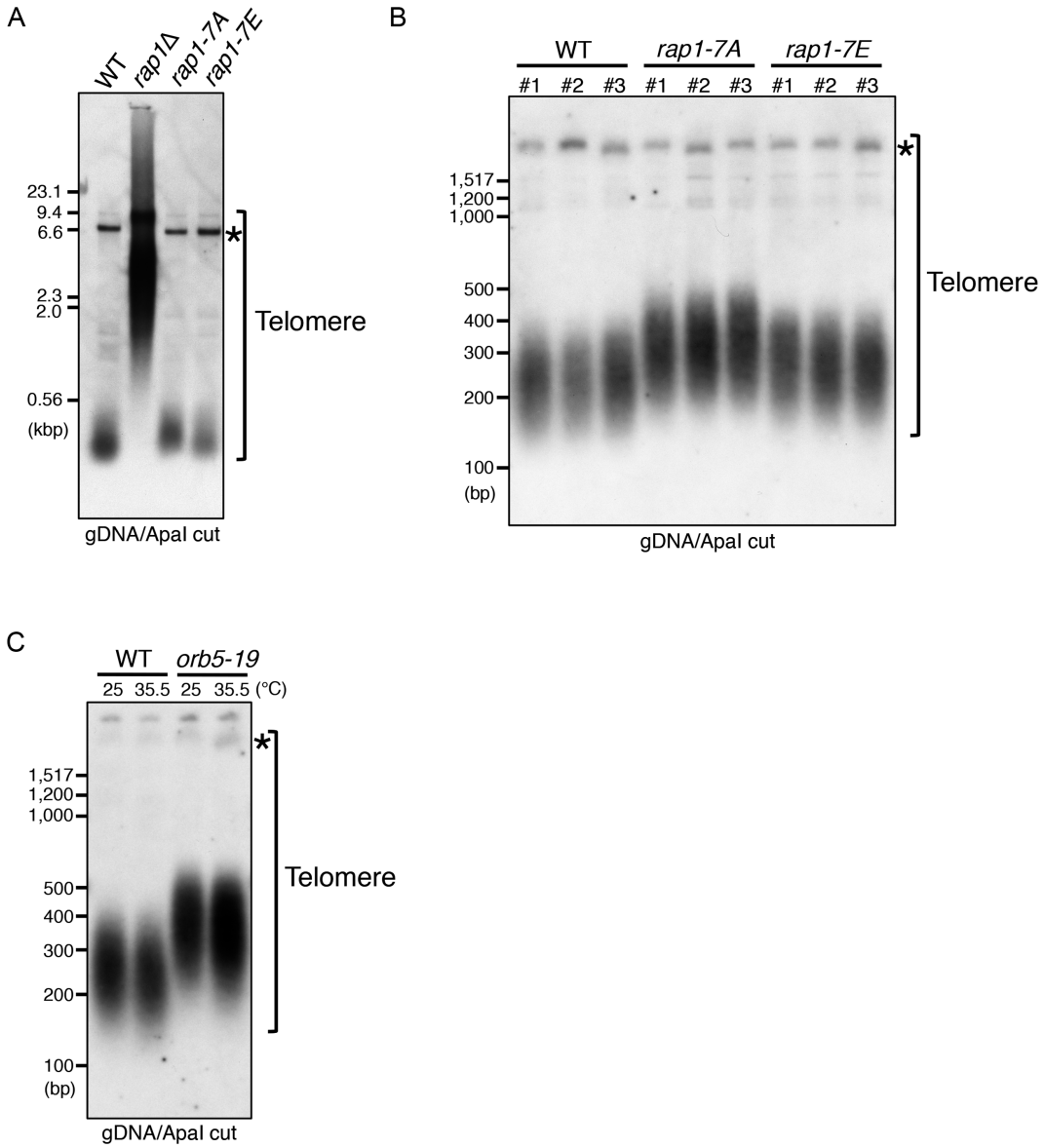

Figure 7. Rap1 phosphorylation by CK2 contributes to the maintenance of normal telomere DNA length. (**A**) Analyses of telomere DNA length of the *rap1-7A* and *rap1-7E* mutants. Cells were grown in YES at 32°C. Genomic DNA was digested with ApaI, separated in a 1% agarose gel and subjected to Southern blot analysis using telomere DNA as a probe. An asterisk indicates the position of telomeres of chromosome 3. (**B**) Analyses of telomere DNA length of the *rap1-7A* and *rap1-7E* mutants with high resolution. Cells were grown in YES at 32°C. Genomic DNA was digested with ApaI, separated in a 3% agarose gel and subjected to Southern blot analysis using telomere DNA as a probe. Three independent clones for each genotype were analyzed. (**C**) The *orb5-19* mutant shows elongated telomere DNA. Cells were grown at 25°C or at 35.5°C for 8 h. Southern blot analyses were performed as in (B).

tachment of telomeres from the NE (i.e. the detachment of Rap1 and Bqt4) or changes in heterochromatin structure. Therefore, our results demonstrate that the Rap1 phosphorylation by CK2 promotes formation of the silenced chromatin at chromosome ends through shelterin complex formation.

DISCUSSION

In this study, we discovered a novel regulatory mechanism of telomere complex formation that requires CK2. We showed that the Rap1 phosphorylation by CK2 promotes two protein–protein interactions, specifically Rap1–Bqt4 and Rap1–Poz1. The former regulates telomere tethering to the NE, whereas the latter mediates the localization of shelterin components to both telomeres and subtelomeres, thereby maintaining telomere DNA length and promoting the formation of silenced chromatin at the chromosome ends (Figure 9A and B).

Unexpectedly, the degree of deficiencies in the telomere functions of the *rap1-7A* mutant varied from; no defect in protection of chromosome ends, through a moderate defect in telomere DNA length control, to severe defects in telomere tethering to the NE and subtelomeric gene silencing. It is possible that the numbers of telomere-binding proteins required for each function are different. Thus, minimal

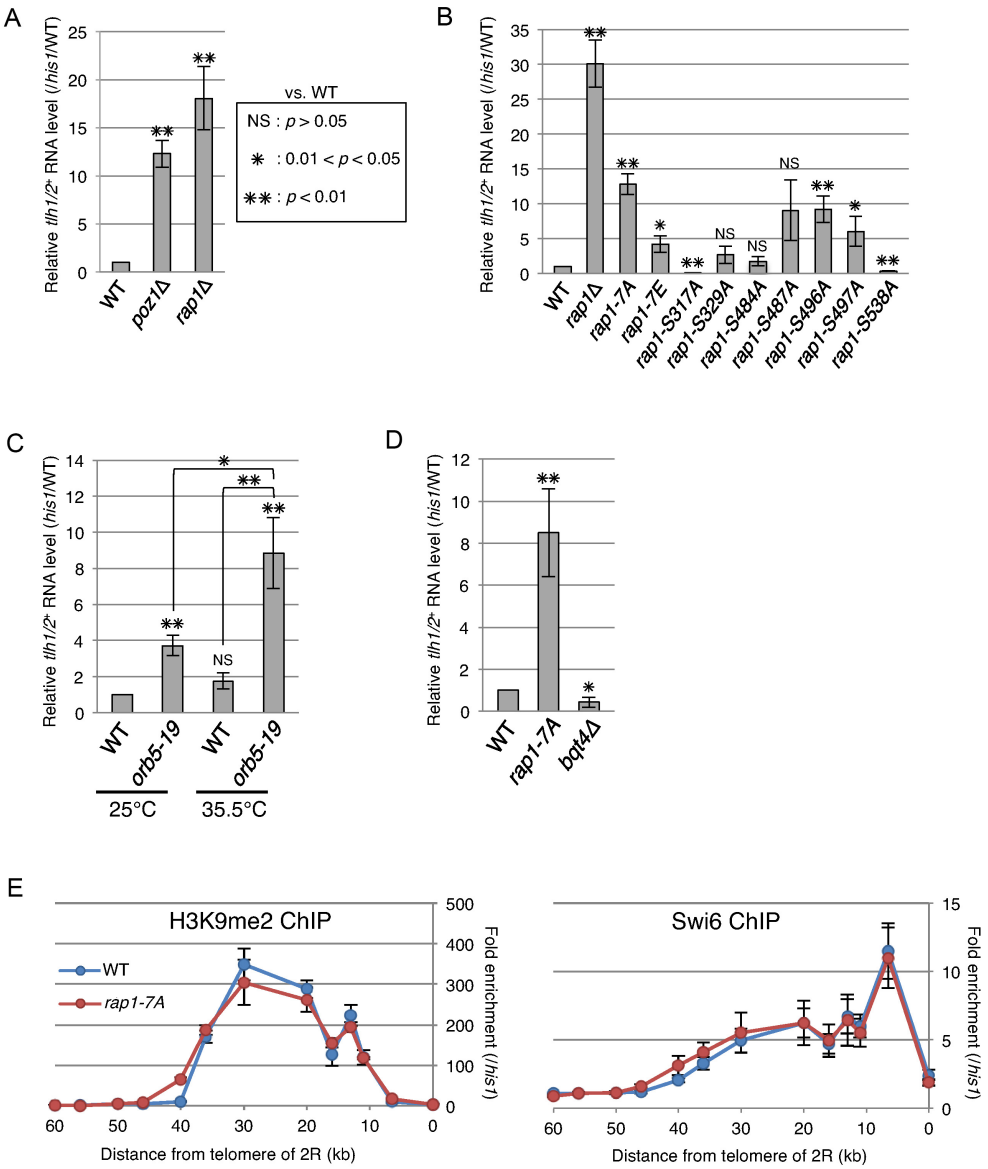

Figure 8. Rap1 phosphorylation by CK2 facilitates the formation of silenced chromatin at chromosome ends. (**A**) Rap1 and Poz1 are required for normal gene silencing at subtelomeres. The RNA level of the *tlh1/2*$^+$ genes was analyzed by qRT-PCR. Expression of *tlh1/2*$^+$ relative to that of *his1*$^+$ was normalized to that in the wild type strain. Error bars indicate the s.d. $N = 3$. *p*, Student's *t*-test (versus wild type). $^{**}p < 0.01$. (**B**) Rap1 phosphorylation by CK2 is required for gene silencing at subtelomeres. RNA expression of the *tlh1/2*$^+$ genes was analyzed as in (A). *p*, Student's *t*-test (versus wild type). NS, $p > 0.05$; $0.01 < {}^*p < 0.05$; $^{**}p < 0.01$. (**C**) Defective subtelomeric gene silencing in the *orb5-19* mutant. Wild-type and *orb5-19* cells were grown in YES at 25°C or at 35.5°C for 8 h. Expression of *tlh1/2*$^+$ relative to that of *his1*$^+$ was normalized to that in the wild type strain at 25°C. *p*, Student's *t*-test (versus wild type or between the strains indicated by bracket lines). NS, $p > 0.05$; $0.01 < {}^*p < 0.05$; $^{**}p < 0.01$. (**D**)The *bqt4*Δ mutant does not show a defect in subtelomeric gene silencing. RNA expression of the *tlh1/2*$^+$ genes was analyzed as in (A). *p*, Student's *t*-test (versus wild type). $0.01 < {}^*p < 0.05$; $^{**}p < 0.01$. (**E**) The *rap1-7A* mutant is not defective in heterochromatin formation. ChIP analyses of histone H3 methylated at K9 and Swi6 at the subtelomere of the right arm of chromosome 2 followed by qPCR. Fold enrichment relative to the *his1* locus is shown. Error bars indicate the s.d. $N = 3$.

numbers of shelterin proteins are sufficient for chromosome end protection. This study has also revealed that shelterin components are localized not only at telomeres but also at subtelomeres to form a silenced chromatin structure. It is currently unknown how Taz1, a telomere DNA-binding protein, associates with subtelomere DNA; the role of subtelomeric shelterin is also obscure. Further analysis will be required to clarify these questions.

This study indicates that of the seven putative phosphorylation sites, the phosphorylation of Ser496 is the most important for the regulation of both Rap1–Bqt4 and Rap1–Poz1 interactions. Ser496 resides within the Bqt4-interacting interface (490–513 a.a.) (29). Although Ser496 lies just outside of the Poz1-interacting interface (467–491 a.a.) (28), the longer region of Rap1 (467–496 a.a.) was required for production of high-quality crystals of the Rap1–Poz1–Tpz1 complex (27), suggesting that phosphorylation of Ser496 can influence the Rap1-Poz1 interaction. The phosphorylation of Ser496 might facilitate Rap1 interactions with Bqt4 and Poz1 through its negative charge, or

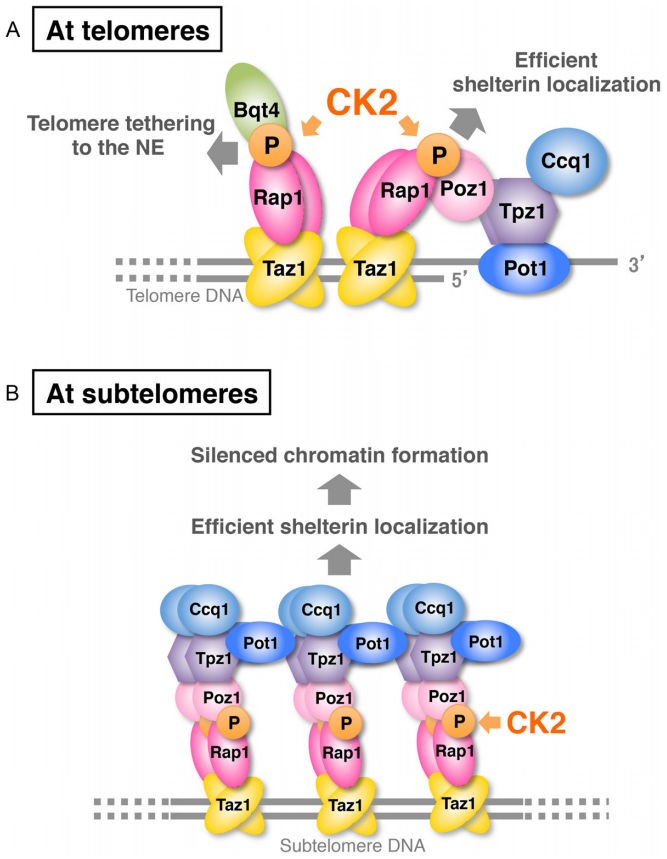

Figure 9. Model of the regulatory mechanisms of CK2-mediated Rap1 phosphorylation. (**A**) Rap1 phosphorylation by CK2 facilitates two interactions, namely Rap1–Bqt4 and Rap1–Poz1 associations. The Rap1–Bqt4 association enables telomere tethering to the NE. The Rap1–Poz1 association is required for the normal localization of shelterin components at telomeres. (**B**) Rap1 phosphorylation by CK2 also facilitates the normal localization of shelterin components to subtelomeres to form a specialized chromatin structure at chromosome ends. It is speculated that most Pot1 proteins at subtelomeres are not linked to the relatively short ss-telomere DNA at chromosome ends, although it is possible that a small portion of Pot1 at subtelomeres binds to ss-telomere DNA.

it might change the three-dimensional structure of Rap1 to expose interaction domains for Bqt4 and Poz1. Further investigation will be required to clarify these possibilities.

The Rap1-Bqt4 and Rap1-Poz1 interactions take place at the same time during interphase. It has been shown that Taz1 forms a homodimer that binds to ds-telomere DNA (36), and that Tpz1, Poz1 and Rap1 form a ternary complex, which forms a dimerized structure (27,28). Therefore, the most likely model is that two molecules of Rap1 bind a homodimer of Taz1 to form a dimer of the ternary Tpz1–Poz1–Rap1 complex (Figure 9A). It is possible that Bqt4 and Poz1 bind to the same Rap1 molecule at the same time because most of the binding interfaces in Rap1 for Poz1 and Bqt4 do not overlap, although they are very close to each other. Another possibility is that Bqt4 binds to Rap1 independently of Poz1.

Our previous study demonstrated that Rap1 is phosphorylated by Cdc2 at Thr378, Ser422 and Ser513 during mitosis (17) (Figure 3A). These phosphorylation events have an inhibitory effect on the Rap1–Bqt4 interaction, which leads to the transient release of telomeres from the NE to ensure precise chromosome segregation (17). Thus, Rap1 phosphorylation events by CK2 and Cdc2 have opposite effects on Rap1–Bqt4 interactions. Among the Cdc2-mediated phosphorylation sites, the phosphorylation of Ser513 is crucial for the dissociation of Rap1 from Bqt4 (17). This study identified Ser496 as the crucial phosphorylation site that promotes Rap1–Bqt4 interactions. Three-dimensional structural analysis of these Rap1 phosphorylation sites (Ser496 and Ser513) and Bqt4 will clarify how the Rap1–Bqt4 interaction is turned on and off.

It has been shown that CK2 plays important roles in chromosome functions. In *S. pombe*, Swi6 (HP1) phosphorylation by CK2 regulates transcriptional gene silencing at pericentromeric heterochromatin regions (15). Thus, it is speculated that Swi6 at subtelomeres is also regulated by CK2. In humans, CK2 phosphorylates and regulates TRF1, a Taz1 homologue (16). Considering that the *orb5-19* mutant showed longer telomere DNA than the *rap1-7A* mutant (Figure 7C), it is therefore possible that CK2 has other phosphorylation targets at telomeres, such as Taz1, and is involved in different aspects of telomere functions in *S. pombe*. In fact, Taz1 contains CK2 consensus phosphorylation sequences. In summary, the formation of telomeric and subtelomeric protein complexes is regulated by multiple phosphorylation reactions. Given that CK2 is constitutively active throughout the cell cycle, the phosphorylation events mediated by CK2 might provide the bases of the formation of various protein complexes with telomere functions. Additional layers of regulation, which are mediated by different protein modifications such as dephosphorylation, ubiquitination, sumoylation, or phosphorylation in neighboring regions, might be responsible for the turnover or deformation of telomere protein complexes during various cellular processes.

SUPPLEMENTARY DATA

Supplementary Data are available at NAR Online.

ACKNOWLEDGEMENTS

We thank M. Tanaka and Y. Takeshita for technical assistance, H. Maekawa and D. Drummond for critical reading of the manuscript, P. Nurse, H. Murakami and National BioResource Project (NBRP) in Japan for the *orb5-19* strains, M. Ueno for technical advices, and all former and present lab members for discussion and support.

FUNDING

Japan Society for the Promotion of Science (JSPS) KAKENHI [16H01310, 26290061, 23114009, 17H03606, 19H05262]; Asahi Glass Foundation, the Mitsubishi Foundation, Daiichi Sankyo Foundation of Life Science, and Ohsumi Frontier Science Foundation (to J.K.). Funding for open access charge: my grant.
Conflict of interest statement. None declared.

REFERENCES

1. de Lange,T. (2005) Shelterin: the protein complex that shapes and safeguards human telomeres. *Genes Dev.*, **19**, 2100–2110.

2. Bianchi,A. and Shore,D. (2008) How telomerase reaches its end: mechanism of telomerase regulation by the telomeric complex. *Mol. Cell*, **31**, 153–165.
3. de Lange,T. (2009) How telomeres solve the end-protection problem. *Science*, **326**, 948–952.
4. Miyoshi,T., Kanoh,J., Saito,M. and Ishikawa,F. (2008) Fission yeast Pot1-Tpp1 protects telomeres and regulates telomere length. *Science*, **320**, 1341–1344.
5. Cooper,J.P., Nimmo,E.R., Allshire,R.C. and Cech,T.R. (1997) Regulation of telomere length and function by a Myb-domain protein in fission yeast. *Nature*, **385**, 744–747.
6. Baumann,P. and Cech,T.R. (2001) Pot1, the putative telomere end-binding protein in fission yeast and humans. *Science*, **292**, 1171–1175.
7. Chikashige,Y. and Hiraoka,Y. (2001) Telomere binding of the Rap1 protein is required for meiosis in fission yeast. *Curr. Biol.*, **11**, 1618–1623.
8. Kanoh,J. and Ishikawa,F. (2001) spRap1 and spRif1, recruited to telomeres by Taz1, are essential for telomere function in fission yeast. *Curr. Biol.*, **11**, 1624–1630.
9. Fujita,I., Tanaka,M. and Kanoh,J. (2012) Identification of the functional domains of the telomere protein Rap1 in *Schizosaccharomyces pombe*. *PLoS ONE*, **7**, e49151.
10. Chikashige,Y., Yamane,M., Okamasa,K., Tsutsumi,C., Kojidani,T., Sato,M., Haraguchi,T. and Hiraoka,Y. (2009) Membrane proteins Bqt3 and -4 anchor telomeres to the nuclear envelope to ensure chromosomal bouquet formation. *J. Cell Biol.*, **187**, 413–427.
11. Chikashige,Y., Tsutsumi,C., Yamane,M., Okamasa,K., Haraguchi,T. and Hiraoka,Y. (2006) Meiotic proteins bqt1 and bqt2 tether telomeres to form the bouquet arrangement of chromosomes. *Cell*, **125**, 59–69.
12. Ahmed,K., Gerber,D.A. and Cochet,C. (2002) Joining the cell survival squad: an emerging role for protein kinase CK2. *Trends Cell Biol.*, **12**, 226–230.
13. Pinna,L.A. (2002) Protein kinase CK2: a challenge to canons. *J. Cell Sci.*, **115**, 3873–3878.
14. Nunez de Villavicencio-Diaz,T., Rabalski,A.J. and Litchfield,D.W. (2017) Protein kinase CK2: intricate relationships within regulatory cellular networks. *Pharmaceuticals (Basel)*, **10**, E27.
15. Shimada,A., Dohke,K., Sadaie,M., Shinmyozu,K., Nakayama,J., Urano,T. and Murakami,Y. (2009) Phosphorylation of Swi6/HP1 regulates transcriptional gene silencing at heterochromatin. *Genes Dev.*, **23**, 18–23.
16. Kim,M.K., Kang,M.R., Nam,H.W., Bae,Y.S., Kim,Y.S. and Chung,I.K. (2008) Regulation of telomeric repeat binding factor 1 binding to telomeres by casein kinase 2-mediated phosphorylation. *J. Biol. Chem.*, **283**, 14144–14152.
17. Fujita,I., Nishihara,Y., Tanaka,M., Tsujii,H., Chikashige,Y., Watanabe,Y., Saito,M., Ishikawa,F., Hiraoka,Y. and Kanoh,J. (2012) Telomere-nuclear envelope dissociation promoted by Rap1 phosphorylation ensures faithful chromosome segregation. *Curr. Biol.*, **22**, 1932–1937.
18. Meggio,F. and Pinna,L.A. (2003) One-thousand-and-one substrates of protein kinase CK2? *FASEB J.*, **17**, 349–368.
19. Moreno,S., Klar,A. and Nurse,P. (1991) Molecular genetic analysis of fission yeast *Schizosaccharomyces pombe*. *Methods Enzymol.*, **194**, 795–823.
20. Bahler,J., Wu,J.Q., Longtine,M.S., Shah,N.G., McKenzie,A., 3rd,Steever, Wach,A.B., Philippsen,A. and Pringle,J.R. (1998) Heterologous modules for efficient and versatile PCR-based gene targeting in *Schizosaccharomyces pombe*. *Yeast*, **14**, 943–951.
21. Forsburg,S.L. and Rhind,N. (2006) Basic methods for fission yeast. *Yeast*, **23**, 173–183.
22. Kanoh,J., Sadaie,M., Urano,T. and Ishikawa,F. (2005) Telomere binding protein Taz1 establishes Swi6 heterochromatin independently of RNAi at telomeres. *Curr. Biol.*, **15**, 1808–1819.
23. Allshire,R.C., Nimmo,E.R., Ekwall,K., Javerzat,J.P. and Cranston,G. (1995) Mutations derepressing silent centromeric domains in fission yeast disrupt chromosome segregation. *Genes Dev.*, **9**, 218–233.
24. Kipling,D. and Kearsey,S.E. (1990) Reversion of autonomously replicating sequence mutations in *Saccharomyces cerevisiae*: creation of a eucaryotic replication origin within procaryotic vector DNA. *Mol. Cell Biol.*, **10**, 265–272.
25. Matsuura,A., Naito,T. and Ishikawa,F. (1999) Genetic control of telomere integrity in *Schizosaccharomyces pombe*: *rad3*$^+$ and *tel1*$^+$ are parts of two regulatory networks independent of the downstream protein kinases *chk1*$^+$ and *cds1*$^+$. *Genetics*, **152**, 1501–1512.
26. Snell,V. and Nurse,P. (1994) Genetic analysis of cell morphogenesis in fission yeast—a role for casein kinase II in the establishment of polarized growth. *EMBO J.*, **13**, 2066–2074.
27. Kim,J.K., Liu,J., Hu,X., Yu,C., Roskamp,K., Sankaran,B., Huang,L., Komives,E.A. and Qiao,F. (2017) Structural basis for shelterin bridge assembly. *Mol. Cell*, **68**, 698–714.
28. Xue,J., Chen,H., Wu,J., Takeuchi,M., Inoue,H., Liu,Y., Sun,H., Chen,Y., Kanoh,J. and Lei,M. (2017) Structure of the fission yeast *S. pombe* telomeric Tpz1-Poz1-Rap1 complex. *Cell Res.*, **27**, 1503–1520.
29. Hu,C., Inoue,H., Sun,W., Takeshita,Y., Huang,Y., Xu,Y., Kanoh,J. and Chen,Y. (2019) Structural insights into chromosome attachment to the nuclear envelope by an inner nuclear membrane protein Bqt4 in fission yeast. *Nucleic Acids Res.*, **47**, 1573–1584.
30. Chen,Y., Rai,R., Zhou,Z.R., Kanoh,J., Ribeyre,C., Yang,Y., Zheng,H., Damay,P., Wang,F., Tsujii,H. *et al.* (2011) A conserved motif within RAP1 has diversified roles in telomere protection and regulation in different organisms. *Nat. Struct. Mol. Biol.*, **18**, 213–221.
31. Liu,J., Yu,C., Hu,X., Kim,J.K., Bierma,J.C., Jun,H.I., Rychnovsky,S.D., Huang,L. and Qiao,F. (2015) Dissecting fission yeast shelterin interactions via MICro-MS links disruption of shelterin bridge to tumorigenesis. *Cell Rep.*, **12**, 2169–2180.
32. Scott,H., Kim,J.K., Yu,C., Huang,L., Qiao,F. and Taylor,D.J. (2017) Spatial organization and molecular interactions of the *Schizosaccharomyces pombe* Ccq1-Tpz1-Poz1 shelterin complex. *J. Mol. Biol.*, **429**, 2863–2872.
33. Timashev,L.A., Babcock,H., Zhuang,X. and de Lange,T. (2017) The DDR at telomeres lacking intact shelterin does not require substantial chromatin decompaction. *Genes Dev.*, **31**, 578–589.
34. Vancevska,A., Douglass,K.M., Pfeiffer,V., Manley,S. and Lingner,J. (2017) The telomeric DNA damage response occurs in the absence of chromatin decompaction. *Genes Dev.*, **31**, 567–577.
35. Sugiyama,T., Cam,H.P., Sugiyama,R., Noma,K., Zofall,M., Kobayashi,R. and Grewal,S.I. (2007) SHREC, an effector complex for heterochromatic transcriptional silencing. *Cell*, **128**, 491–504.
36. Spink,K.G., Evans,R.J. and Chambers,A. (2000) Sequence-specific binding of Taz1p dimers to fission yeast telomeric DNA. *Nucleic Acids Res.*, **28**, 527–533.
37. Agard,D.A., Hiraoka,Y., Shaw,P. and Sedat,J.W. (1989) Fluorescence microscopy in three dimensions. *Methods Cell Biol.*, **30**, 353–377.